


## Article

# Ubiquitin Ligase Nrdp1 Controls Autophagy-Associated Acrosome Biogenesis and Mitochondrial Arrangement during Spermiogenesis

Zi-Yu Luo <sup>1,†</sup>, Tian-Xia Jiang <sup>1,†</sup> , Tao Zhang <sup>2</sup>, Ping Xu <sup>2,\*</sup> and Xiao-Bo Qiu <sup>1,\*</sup>

<sup>1</sup> Ministry of Education Key Laboratory of Cell Proliferation & Regulation Biology, College of Life Sciences, Beijing Normal University, 19 Xijiekouwai Avenue, Beijing 100875, China; 201111201017@mail.bnu.edu.cn (Z.-Y.L.); jiangtx@bnu.edu.cn (T.-X.J.)

<sup>2</sup> State Key Laboratory of Proteomics, Beijing Proteome Research Center, Institute of Lifeomics, 38 Science Park Road, Beijing 102206, China; zhangtao120567648@163.com

\* Correspondence: xuping@ncpsb.org.cn (P.X.); xqiu@bnu.edu.cn (X.-B.Q.)

† These authors contributed equally to this work.

**Abstract:** Autophagy is critical to acrosome biogenesis and mitochondrial quality control, but the underlying mechanisms remain unclear. The ubiquitin ligase Nrdp1/RNF41 promotes ubiquitination of the mitophagy-associated Parkin and interacts with the pro-autophagic protein SIP/CacyBP. Here, we report that global deletion of Nrdp1 leads to formation of the round-headed sperm and male infertility by disrupting autophagy. Quantitative proteome analyses demonstrated that the expression of many proteins associated with mitochondria, lysosomes, and acrosomes was dysregulated in either spermatids or sperm of the Nrdp1-deficient mice. Deletion of Nrdp1 increased the levels of Parkin but decreased the levels of SIP, the mitochondrial fission protein Drp1 and the mitochondrial protein Tim23 in sperm, accompanied by the inhibition of autophagy, the impairment of acrosome biogenesis and the disruption of mitochondrial arrangement in sperm. Thus, our results uncover an essential role of Nrdp1 in spermiogenesis and male fertility by promoting autophagy, providing important clues to cope with the related male reproductive diseases.

**Keywords:** ubiquitin ligase; Nrdp1; Parkin; SIP/CacyBP; autophagy; acrosome; mitochondrion; mitophagy; spermiogenesis



**Citation:** Luo, Z.-Y.; Jiang, T.-X.; Zhang, T.; Xu, P.; Qiu, X.-B. Ubiquitin Ligase Nrdp1 Controls Autophagy -Associated Acrosome Biogenesis and Mitochondrial Arrangement during Spermiogenesis. *Cells* **2023**, *12*, 2211. <https://doi.org/10.3390/cells12182211>

Academic Editor: Hengbin B. Wang

Received: 15 June 2023

Revised: 23 July 2023

Accepted: 27 July 2023

Published: 5 September 2023



**Copyright:** © 2023 by the authors. Licensee MDPI, Basel, Switzerland. This article is an open access article distributed under the terms and conditions of the Creative Commons Attribution (CC BY) license (<https://creativecommons.org/licenses/by/4.0/>).

## 1. Introduction

Spermiogenesis is the final phase of spermatogenesis characterized by condensation of DNA, replacement of nucleosomal histones with protamines, development of acrosome, and formation of the sperm tail connected with a mitochondria-rich midpiece [1,2]. The acrosome, located in the anterior part of the sperm nucleus, is a membranous lysosome-related organelle (LRO) [3,4]. Acrosome contains proteolytic enzymes that help sperm to enter an egg and is indispensable for fertilization [5]. Macroautophagy (hereafter referred to as autophagy) is an evolutionarily conserved process that degrades cellular proteins and damaged or excessive organelles. In this process, the double-membraned autophagosome fuses with lysosomes to form autolysosomes, where autophagic cargoes are degraded [6,7]. Formation of the autophagosome and selective recruitment of certain cargoes require LC3-II, whose precursor can be cleaved by ATG4 to form cytoplasmic LC3-I. LC3-I is then conjugated to phosphatidylethanolamine to form LC3-II on the phagophore membrane [8,9]. Mitophagy is an autophagic process to remove damaged or excessive mitochondria with induction of autophagy and recruitment of mitochondria [10]. Autophagy is critical to acrosome biogenesis [11], while mitophagy is important for mitochondrial organization in sperm [12]. However, how these processes are executed and regulated remains unclear.

The ubiquitin–proteasome pathway degrades most cellular proteins, and its dysregulation is involved in various diseases, including cancer and neurodegenerative diseases [13].

Inhibitors of the proteasome were widely used in the clinical treatment of multiple myeloma and mantle cell lymphoma [14]. The ubiquitin ligase Nrdp1/RNF41 regulates cell growth, apoptosis, and autophagy by promoting ubiquitination of multiple important substrates, including the epidermal growth factor receptor family member ErbB3/HER3 [15], the pro-autophagic factor SIP/CacyBP [16], the dual inhibitor of apoptosis and autophagy BIRC6/BRUCE [16,17] and the mitophagy-associated ubiquitin ligase Parkin [18]. Parkin can maintain mitochondrial quality by promoting mitophagy [19]. Drp1 plays an important role in Parkin-mediated mitophagy by promoting mitochondrial fission [20,21]. Recently, we showed that Nrdp1 promotes monoubiquitination of SIP/CacyBP, enhances its association with Rab8, BIRC6, and LC3-I in the trans-Golgi network, and thus facilitates autophagosome formation and autophagic degradation of BIRC6 [16]. Nrdp1 is highly expressed in the testis, pancreas, brain, and muscles [15,22]. To understand the physiological roles of Nrdp1, we generated the mice with global deletion of Nrdp1 and found that the Nrdp1-deficient male mice are infertile with impaired spermiogenesis. Notably, our results suggest that Nrdp1 controls the mitochondrial arrangement in sperm and acrosome biogenesis by promoting autophagy.

## 2. Materials and Methods

### 2.1. Mice

Construction of the Nrdp1-deficient mice was achieved by Biocytogen Pharmaceuticals Co., Ltd. (Beijing, China). Mice were kept in the Institute of Brain and Cognitive Sciences, Beijing Normal University using standard humane animal husbandry protocols. The animals' care was in accordance with institutional guidelines. Unless stated elsewhere, mice were 6 per group with age- and sex-matched in each experiment. Sample size was based on empirical data from pilot experiments. No additional randomization or blinding was used to allocate experimental groups. For genotyping, DNA was extracted from the tip of the tail and analyzed by PCR with the primers: wild-type: 5'-CCACACGCAGCCCTCGTACTC (forward), 5'-AGGTCCAGGGCTACAATCAAGG (reverse); Nrdp1-deficient: 5'-CCACACGCAGCCCTCGTACTC (forward), and 5'-CCAGCACCTGCCA CGGATT (reverse).

### 2.2. Antibody Information

The antibody for Sp56 was kindly gifted from Prof. Fei Gao. Other antibodies were purchased according to the following information: Afaf (Abcam, Cambridge, UK, ab121470); Drp1 (BD bioscience, Franklin Lakes, NJ, USA, 611113); GM130 (Abcam, ab52649); LAMP1 (Sigma-Aldrich, St. Louis, MO, USA, L1418); LC3B (Sigma-Aldrich, L7543); Nrdp1 (Santa Cruz Biotechnology, Dallas, TX, USA, sc-365622); OPTN (Proteintech, Rosemont, IL, USA, 10837-1-A); Parkin (Sigma-Aldrich, P6248); p62 (Cell Signaling Technology, Danvers, MA, USA, 88588); SIP/CacyBP (Santa Cruz, sc-166455); Sox9 (Abcam, ab185966); Tim23 (BD bioscience; 611222); VAMP8 (Abcam, ab76021); Ubiquitin (Cell Signaling Technology, 3936S); and  $\beta$ -actin (Sigma-Aldrich, A5441). Peroxidase-conjugated anti-mouse IgG (ZSGB-BIO, Beijing, China, ZB-5305, 1:5000), anti-rat IgG (ZSGB-BIO, ZB-2307, 1:4000), or anti-rabbit IgG (ZSGB-BIO, ZB-5301, 1:3000) was used as the secondary antibody. The protein bands were visualized using the ECL detection system (Millipore, Burlington, MA, USA).

### 2.3. Immunoblotting

Unless stated elsewhere, testes and sperm were homogenized in the buffer containing 20 mM Tris-HCl (pH 8.0), 100 mM KCl, 1 mM EDTA, 1 mM EGTA, 1% Triton X-100, 2.5 mM sodium pyrophosphate, 1 mM  $\beta$ -sodium glycerophosphate and protease inhibitors, sonicated twice at 200 W for 10 s each, and then cleared by centrifugation. For the detection of sperm ubiquitination, we used 1.2 $\times$  SDS sample buffer as a lysis buffer to denature deubiquitinating enzymes and the ubiquitinated proteins. Proteins were separated by SDS-PAGE. After proteins were transferred to a PVDF membrane (Millipore), the blot was

incubated with the indicated primary antibodies. The secondary antibody was goat against rabbit or mouse IgGs conjugated to horseradish peroxidase (HRP).

#### 2.4. Tissue Collection and Immunostaining

Testes were fixed in 4% paraformaldehyde (PFA) at 4 °C overnight, dehydrated, embedded in paraffin, and sectioned at 5 µm. The sections were de-paraffinized, rehydrated, and followed by antigen retrieval in 10 mM of the sodium citrate buffer. Then, sections were blocked with goat serum in 0.3% triton X-100 and incubated with primary antibodies. In the case of a sperm smear, the section can be blocked directly and incubated with primary antibodies. The secondary antibody was goat against rabbit or mouse IgGs conjugated to FITC, and DAPI was used to stain the nuclei of cells.

#### 2.5. Hematoxylin and Eosin (H&E) Staining

Mouse testis and epididymis were excised and fixed in 4% paraformaldehyde overnight. Sectioned at 5 µm and stained by hematoxylin and eosin. The cytoplasm was stained by eosin (red), and the nucleus was stained by hematoxylin (blue).

#### 2.6. Separation of Testis Haploid Cells by Flow Cytometry

Testis dissociation and cell collection were based on a recently described method [23]. Testicles were isolated, de-capsulated, and incubated in the solution containing 1 mg/mL of collagenase, 0.5 mg/mL DNase I, and 1 mg/mL hyaluronidase. The tube was incubated for 10 min at 37 °C, and then seminiferous tubules were incubated in pre-heated solution with 1 mg/mL of collagenase, 0.5 mg/mL DNase I, and 1 mg/mL trypsin for 10 min at 37 °C. The tubules were gently pipetted up and down. The suspension was passed through a 100 µm nylon cell strainer and washed with 1× PBS. The cells were then incubated with Hoechst33342. The cells were finally sorted by a flow cytometer (BD FACSAria™ III) and analyzed using BD FACSDiva™. Haploid cells were collected based on Hoechst33342 fluorescence intensity.

#### 2.7. Mass Spectrometry

Protein samples were collected from sperm and testis haploid cells of heterozygous deletion of *Nrdp1* (*Nrdp1*<sup>+/-</sup>) and *Nrdp1*-deficient (*Nrdp1*<sup>-/-</sup>) mice, and analyzed for differentially expressed proteins by mass spectrometry at Beijing Proteome Research Center using the methods described previously [24,25]. Briefly, the protein samples were assayed for quality. Equal amounts of each group were taken for protein alkylation and trypsin digestion to obtain peptides. Then, the peptides were labeled with 8-channel Tandem Mass Tag (TMT) reagents, equilibrated, desalted, and cleaned up for the Liquid Chromatography–Mass Spectrometry/Mass Spectrometry (LC-MS/MS) analysis and quantitative studies. The fold changes between the two groups were calculated by dividing the average abundance values of each protein in KO samples by the ones in the control group. The threshold value of proteins upregulated was 1.5, and the downregulated value was 0.67.

#### 2.8. Pathway and Process Enrichment Analyses

For GO term pathway and process enrichment, the analysis has been separately carried out using the “micro-bioinformatics” Gene Annotation and Analysis Resource ([https://www.bioinformatics.com.cn/plot\\_basic\\_gopathway\\_enrichment\\_bubbleplot\\_081](https://www.bioinformatics.com.cn/plot_basic_gopathway_enrichment_bubbleplot_081), accessed on 29 July 2023). We choose our differentially expressed proteins in *Nrdp1*<sup>-/-</sup> testis haploid cells and sperm and obtain a bubble plot.

#### 2.9. Quantification and Statistical Analysis

Unless stated elsewhere, significance levels for comparisons between two groups were determined by a two-tailed unpaired *t*-test, mean and s.e.m. (\* *p* < 0.05, \*\* *p* < 0.01, and \*\*\* *p* < 0.001), and normal distribution. All of the images were chosen blindly and randomly and quantitated by image J (V1.8.0).

### 3. Results

#### 3.1. Global Deletion of *Nrdp1* Leads to Male Infertility

To investigate the physiological role of *Nrdp1*, we generated the mutant mice with global deletion of the *Nrdp1* gene by using Clustered Regularly Interspaced Short Palindromic Repeats (CRISPR)–Cas9 technology (Figure 1A). *Nrdp1* has 7 exons with the translated region stretching across exons 3–7. In this study, the cut sites by Cas9 are located on both sides of exon 4 of *Nrdp1*, resulting in the cleavage of the main region of *Nrdp1* mRNA and loss of *Nrdp1* protein. PCR analyses of genomic DNA indicated that the whole exon 4 has been cut off (Figure S1). Further confirmation of the successful deletion of *Nrdp1* was carried out by immunoblotting in different organs, such as the testis, kidney, and spleen, and the results showed that the *Nrdp1*-deficient mice (*Nrdp1*<sup>−/−</sup>) have been constructed successfully (Figure 1B). Homozygous deletion of *Nrdp1* caused male infertility, and none of the females that bred with *Nrdp1*<sup>−/−</sup> males were pregnant. But *Nrdp1*<sup>−/−</sup> females could produce offspring normally with similar-sized litters as their wild-type or heterozygous littermates (Figure 1C). Intriguingly, there were no significant differences in the volume and weight of testicles (Figure 1D). In addition, no obvious defects were found in spermatogonia, spermatocytes, round spermatids, and elongated spermatids within the seminiferous tubules of *Nrdp1*<sup>−/−</sup> mice as examined by hematoxylin–eosin (HE) staining (Figure 1E). No difference in the *Nrdp1*-deficient Sertoli cells in testes as marked by *Sox9* was observed (Figure S2). On the other hand, no defects were observed in the ovaries, uterus, and follicular cells in the *Nrdp1*-deficient female mice (Figure 1F,G). These results suggest that *Nrdp1* deficiency leads to male infertility probably due to the impaired spermatogenesis after spermatid elongation.

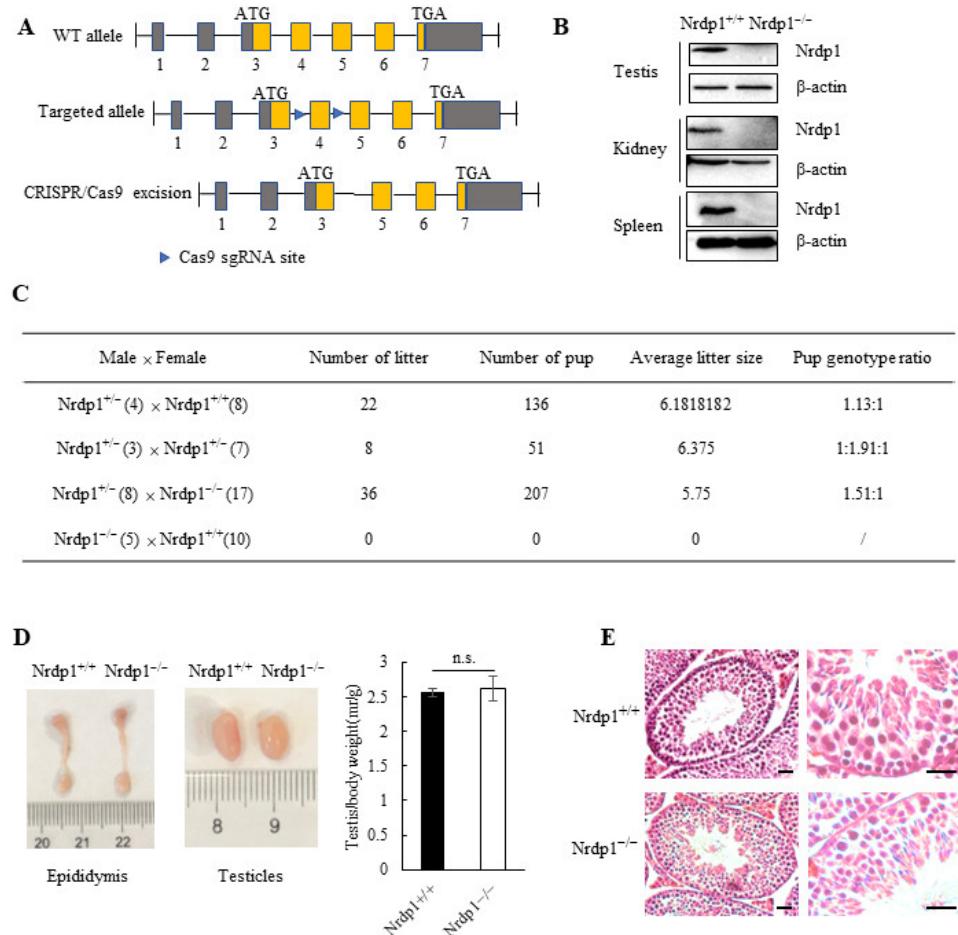
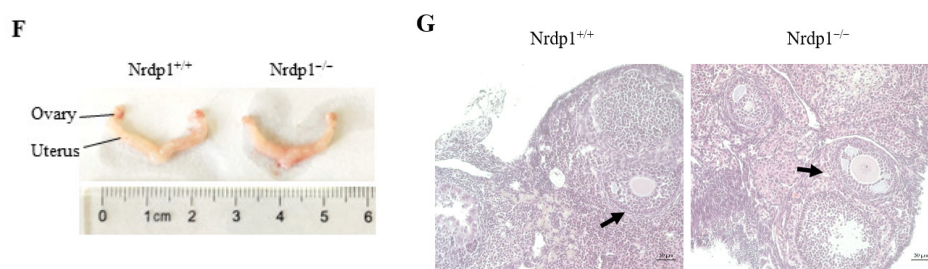


Figure 1. Cont.



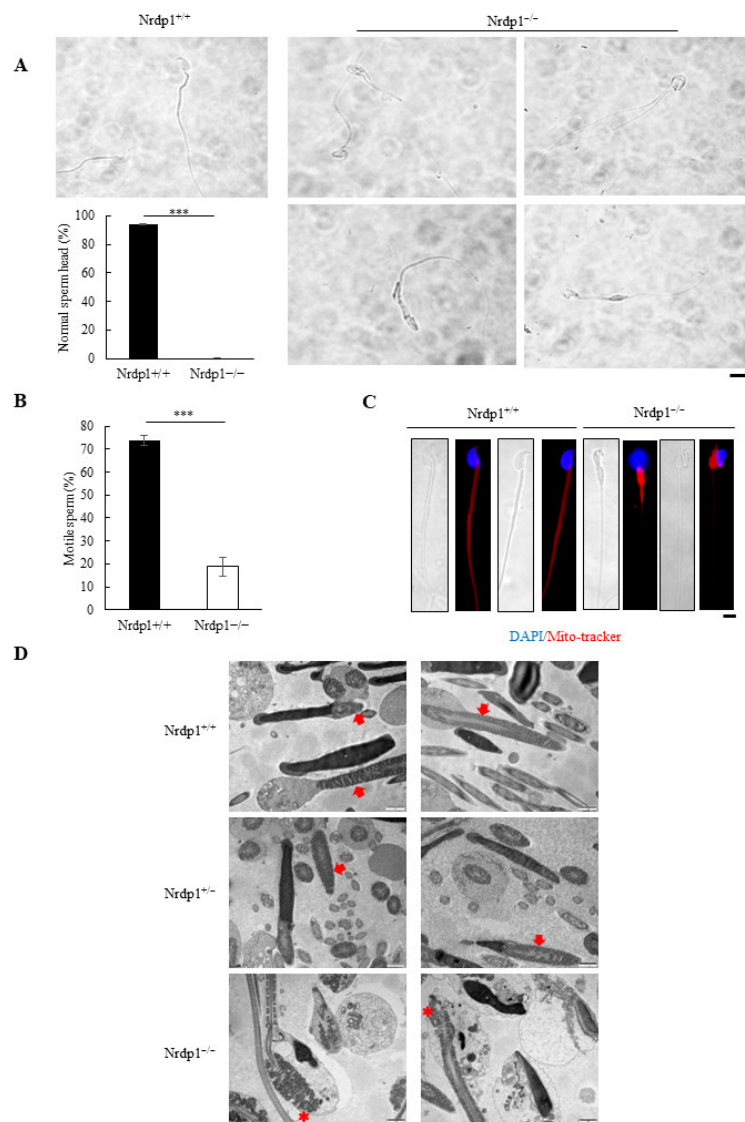
**Figure 1.** Deletion of *Nrdp1* leads to male infertility in mice. (A) Schematic diagram of *Nrdp1* deletion in mice. The sgRNAs were designed to target two flanks between the exon 4 of *Nrdp1* gene. The sequence alignment indicated a 1037 bp loss (including the whole exon 4) that led to the frameshift mutation. WT, the wild-type. (B) Immunoblotting for *Nrdp1* protein in the wild-type (*Nrdp1*<sup>+/+</sup>) and the *Nrdp1*-deficient (*Nrdp1*<sup>-/-</sup>) male tissues, including testes, spleens, and kidneys.  $\beta$ -actin was used as the loading control. (C) Fertility test of *Nrdp1*<sup>-/-</sup> males and females. Adult males of *Nrdp1*<sup>+/-</sup> or *Nrdp1*<sup>-/-</sup> genetic background were mated to *Nrdp1*<sup>+/+</sup>, *Nrdp1*<sup>+/-</sup> or *Nrdp1*<sup>-/-</sup> females. The number of mating mice was indicated in parentheses. The number of litters and pups was recorded for more than two months. (D) The size of the testes and epididymis from *Nrdp1*<sup>+/+</sup> and *Nrdp1*<sup>-/-</sup> male mice.  $n = 4$ . (E) The morphology of the seminiferous tubules from *Nrdp1*<sup>+/+</sup> and *Nrdp1*<sup>-/-</sup> mice was examined by H&E staining. Scale bar = 50  $\mu$ m. (F) The morphology of the ovary and uterus from *Nrdp1*<sup>+/+</sup> and *Nrdp1*<sup>-/-</sup> mice was shown. (G) The morphology of the follicular cells from *Nrdp1*<sup>+/+</sup> and *Nrdp1*<sup>-/-</sup> mice was examined by H&E staining. Black arrow indicating follicles. Scale bar = 50  $\mu$ m. Data are presented as mean  $\pm$  SEM. n.s. stands for not significant. Data are from four independent biological replicates of the same experiment (two-tailed unpaired *t*-test in (D)).

### 3.2. *Nrdp1* Deficiency Causes Round-Headed Sperm with Disrupted Mitochondrial Arrangement

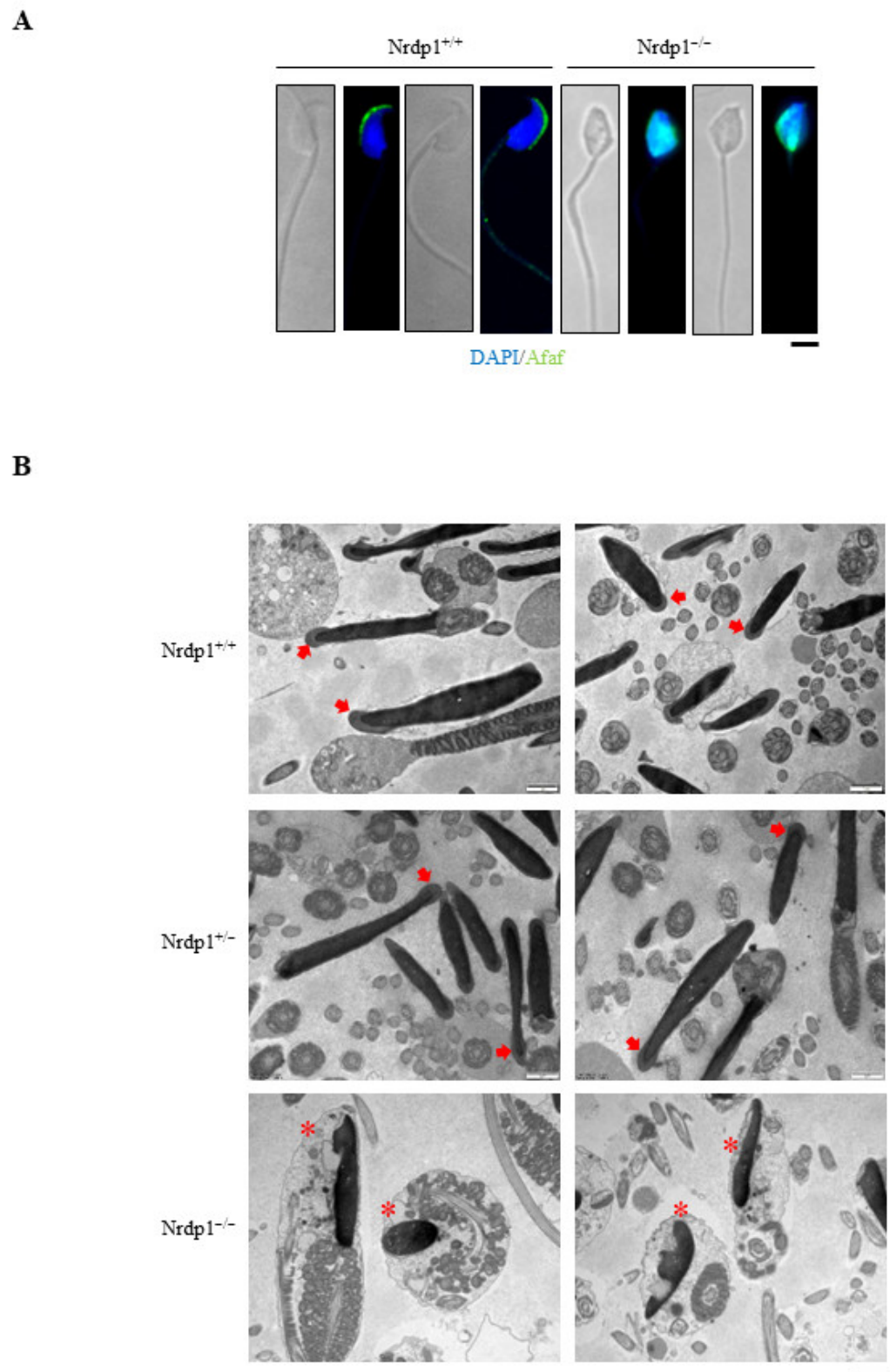
We next analyzed sperms in the mouse epididymis. The heads of almost all sperm in the epididymis of *Nrdp1*<sup>-/-</sup> mice were round, unlike the sickle shape in the wild-type mice (Figure S3A). But the sperm count was not significantly affected in the *Nrdp1*<sup>-/-</sup> mice (Figure S3B). In addition, more than 50% of *Nrdp1*<sup>-/-</sup> sperm had multiple tails and swollen middle pieces of the tail (Figure 2A) with a sharp decrease in sperm motility (Figure 2B and S3C). Accordingly, mitochondria failed to align in the tail but accumulated in the head in *Nrdp1*<sup>-/-</sup> sperm (Figure 2C). Transmission electron microscopy with epididymis sections further confirmed mitochondrial defects with the abnormal structure of mitochondria in *Nrdp1*<sup>-/-</sup> sperm. The structure of mitochondria in the sperm head was mostly abnormal in *Nrdp1*<sup>-/-</sup> samples (Figure 2D). Thus, *Nrdp1* deficiency causes round-headed sperm and disrupts mitochondrial arrangement in sperm, leading to the sharply reduced motility of sperm.

Acrosome formation is a multiple-step process, including Golgi, cap, acrosome, and maturation phases [5]. Immunostaining assay with the acrosome membrane protein Afaf [26] showed that the shape of the sperm head was severely disrupted in the *Nrdp1*<sup>-/-</sup> mice in comparison to the regular sickle shape in the wild-type (Figure 3A). Transmission electron microscopy analyses with epididymis sections further showed nuclear and acrosomal defects in *Nrdp1*<sup>-/-</sup> sperm. Acrosomes were absent or malformed in most *Nrdp1*<sup>-/-</sup> sperm. At the same time, their nuclei were smaller (Figure 3B). To figure out which stages were impaired during acrosome formation, the Golgi phase was visualized by an antibody against the Golgi matrix protein GM130, while the cap, acrosome, and maturation phases were marked with the acrosome-specific protein Afaf. In the Golgi phase, there was no difference in Golgi or proacrosomal vesicles between *Nrdp1*<sup>+/+</sup> and *Nrdp1*<sup>-/-</sup> spermatids. In the cap phase, the length of acrosome anchoring nuclei in *Nrdp1*<sup>-/-</sup> spermatids was much shorter than that in the wild-type. The disordered distribution of acrosomes occurred in both acrosome and maturation phases in *Nrdp1*<sup>-/-</sup> spermatids (Figure 4A). Under a transmission electron microscope, the acrosomes in the Golgi phase were larger and slightly invaginated toward the nucleus in *Nrdp1*<sup>-/-</sup> spermatids (Figure 4B). In the cap phase, the acrosomes of *Nrdp1*<sup>+/+</sup> and *Nrdp1*<sup>+/-</sup> sperm were intact and anchoring tightly to

the nucleus, with a length close to half of the nucleus perimeter, while the acrosomes of  $Nrdp1^{-/-}$  spermatids were shorter with a length of about only one-third of the nucleus perimeter (Figure 4B). In the acrosome phase, the manchette microtubule is the major factor shaping nuclei of the acrosome during the early elongation phase of spermiogenesis [27]. However, the structure of the manchette was dramatically disturbed in the acrosome phase of  $Nrdp1^{-/-}$  spermatids. In the mature phase, the acrosome was not located anteriorly, and small vacuoles appeared in  $Nrdp1^{-/-}$  spermatids (Figure 4B). Thus,  $Nrdp1$  deletion markedly impairs the development of acrosomes in the late phases of acrosome formation.



**Figure 2.**  $Nrdp1^{-/-}$  mice display structural defects in sperm. (A) Single sperm image for the morphology of  $Nrdp1^{+/+}$  (left panel) and  $Nrdp1^{-/-}$  sperm (right panel) derived from cauda epididymis. The percentage of normal or round-headed sperm between  $Nrdp1^{+/+}$  and  $Nrdp1^{-/-}$  mice was calculated. At least 10 random sections were counted. Scale bar = 10  $\mu$ m. (B) The percentage of motile sperm between  $Nrdp1^{+/+}$  and  $Nrdp1^{-/-}$  mice.  $n = 4$ . (C) Fluorescence staining of single sperm using mito-tracker (red), which labeled mitochondrial sheath in the mid-piece of the sperm tail. The nuclei were stained by DAPI (blue). Scale bar = 10  $\mu$ m. (D) The ultrastructure of mitochondria (indicated by arrows in  $Nrdp1^{+/+}$ ,  $Nrdp1^{+/-}$  mice and asterisks in  $Nrdp1^{-/-}$  mice) in sperm using TEM. Scale bar = 1  $\mu$ m. Data are presented as mean  $\pm$  SEM. \*\*\*  $p < 0.001$ . Data are from four independent biological replicates of the same experiment (two-tailed unpaired  $t$ -test in (A,B)).



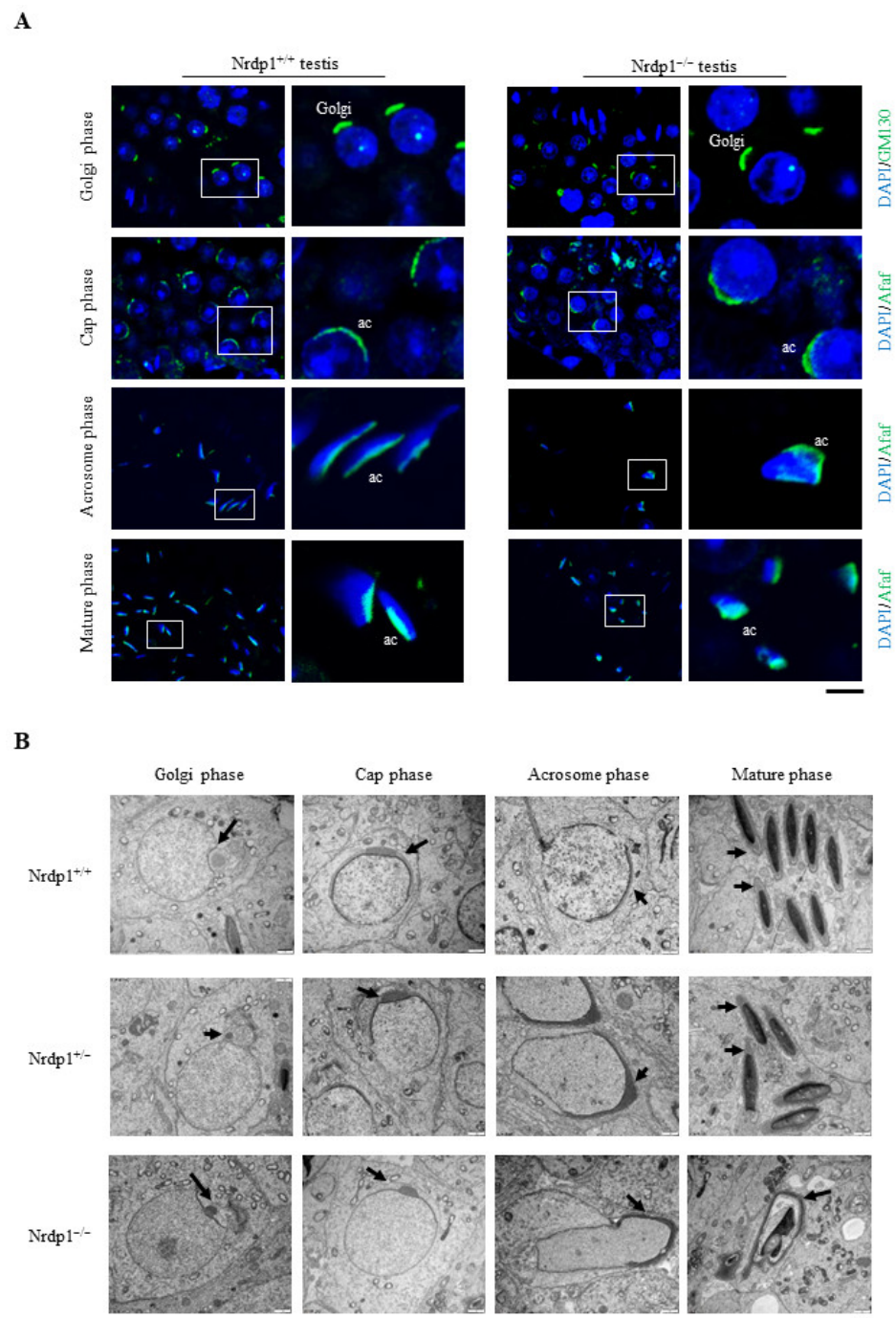


**Figure 4.** Acrosome formation is disrupted in *Nrdp1*-deficient mice. **(A)** Adult testis sections from *Nrdp1*<sup>+/+</sup> and *Nrdp1*<sup>-/-</sup> samples were visualized by the antibody against the Golgi marker GM130 (green). Acrosome membrane protein Afaf (green) was used to label developing acrosome, and DAPI was for nuclei (blue). In the cap phase, both *Nrdp1*<sup>+/+</sup> and *Nrdp1*<sup>-/-</sup> round spermatids display the characteristic acrosomal caps that covered the nuclei. In the acrosome phase, Afaf-labelled acrosome elongated along with cell nuclei in *Nrdp1*<sup>+/+</sup> testis samples, whereas Afaf staining appeared disarranged in *Nrdp1*<sup>-/-</sup> elongated spermatids. ac, acrosome. Scale bar = 10  $\mu$ m. **(B)** The ultrastructure of the Golgi phase showed the proacrosomal granule (arrows) around the nucleus in *Nrdp1*<sup>+/+</sup>, *Nrdp1*<sup>+/-</sup> and *Nrdp1*<sup>-/-</sup> round spermatids. As in *Nrdp1*<sup>+/+</sup> spermatids, acrosomes (arrows) extended along the nucleus in *Nrdp1*<sup>-/-</sup> round spermatids during the cap phase. In the acrosome phase and the mature phase, irregularly shaped acrosomes (arrows) were shown in *Nrdp1*<sup>-/-</sup> elongated spermatids. Scale bar = 1  $\mu$ m. Data are from two independent biological replicates of the same experiment.



### 3.3. *Nrdp1* Deficiency Disrupts Expressions of Lysosomal and Mitochondrial Proteins in Spermatids and Sperm

To explore the mechanisms by which *Nrdp1* regulates spermiogenesis, we performed the TMT-labeled quantitative proteome analysis. Haploid spermatids and immature sperm in mouse testes were stained in nuclei with Hoechst33342 and sorted by a fluorescence-activated cell sorter (FACS), while the late-stage or mature sperm were isolated from mouse epididymis (Figure 5A,B). There were 440 upregulated and 201 downregulated differentially expressed proteins in the *Nrdp1*-deficient (*Nrdp1*<sup>-/-</sup>) testis haploid cells in comparison with the control samples from the mice with the heterozygous deletion of *Nrdp1* (*Nrdp1*<sup>+/-</sup>) (Figure 5C,D), which showed no defects in spermiogenesis. In the *Nrdp1*-deficient epididymis sperm, there were 374 upregulated and 113 downregulated differentially expressed proteins (Figure 5E,F). Eighteen proteins, which were mostly transmembrane proteins, were co-upregulated in the *Nrdp1*-deficient testis and epididymis samples (Figure 5G and Table S1). Three proteins (*Cyp2b10*, *Fam96b*, and *Tmem263*) were upregulated in testes, but downregulated in epididymis samples (Figure 5H and Table S2). *Ints12* was the only one downregulated in both testis and epididymis samples (Figure 5I). Apparently, the deletion of *Nrdp1* led to more proteins being upregulated in both testis and epididymis samples, consistent with the role of *Nrdp1* in ubiquitination, which regulates protein degradation through both proteasomes and lysosomes [28–30]. These results also suggest that *Nrdp1* might play relatively distinct roles in immature haploid cells, including round spermatids, elongated spermatids, and immature sperm in the testis, and the mature sperm characterized with the well-oriented mitochondria and acrosome in the epididymis, supporting a critical role of *Nrdp1* in sperm maturation.

Lysosomal proteins were found highly upregulated in the *Nrdp1*<sup>-/-</sup> testis haploid cells using KEGG pathway analyses (Figure 6A). In addition, sixteen mitochondrial function-related proteins were upregulated in the *Nrdp1*-deficient haploid cells from the testes (Table S3). Contrary to the results from testis samples, the deletion of *Nrdp1* caused the lysosome pathway to downregulate in the *Nrdp1*<sup>-/-</sup> sperm from the epididymis (Figure 6B). The GO term analyses showed that proteins in mitochondria and transport vesicles were ranked at the top as upregulated proteins in the *Nrdp1*-deficient epididymis sperm (Figure 6C and Figure S4A). Among them, the mitochondrial autophagy-related Parkin (*Park2*) [31], the lysosomal membrane protein *LAMP1* [32], and 35 proteins involved in mitochondrial ATP synthesis or NADH dehydrogenase were all upregulated (Table S4). In contrast, multiple acrosome-associated proteins were downregulated in the *Nrdp1*-deficient haploid cells from testes and sperm in the epididymis (Figure 6D and S4B; Tables S5 and S6).

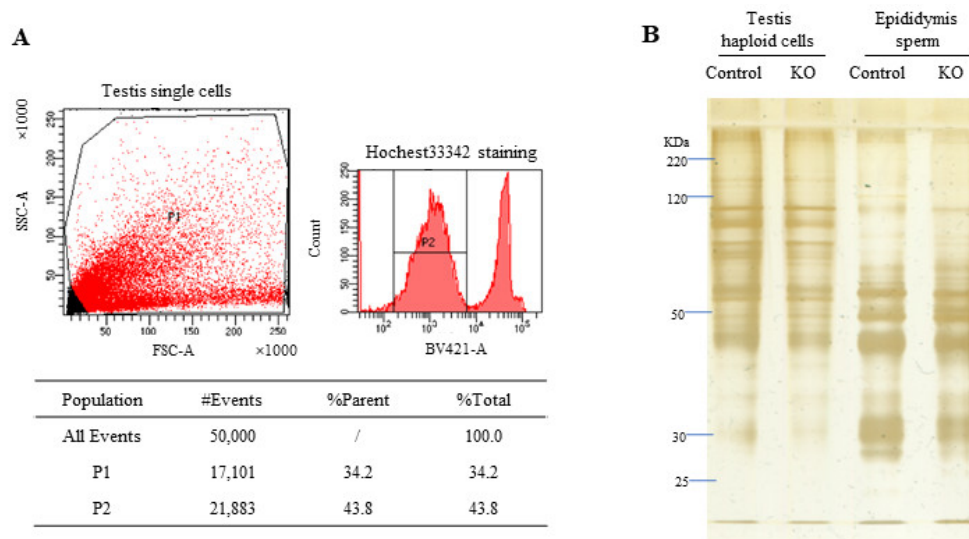
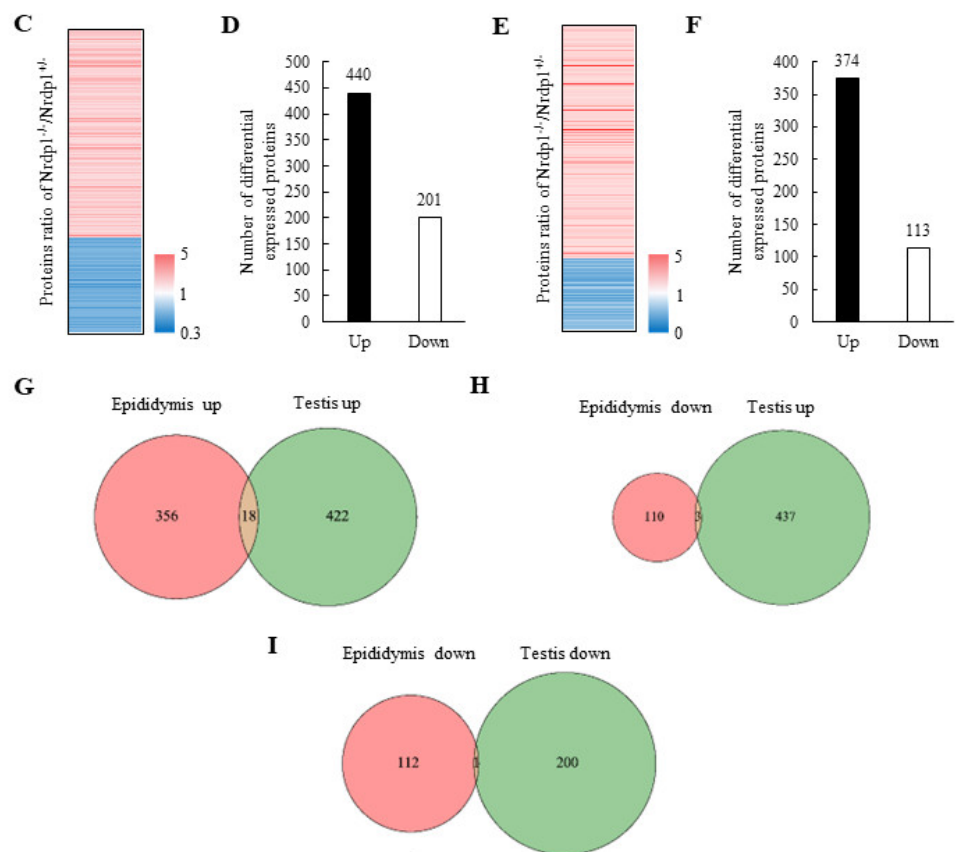
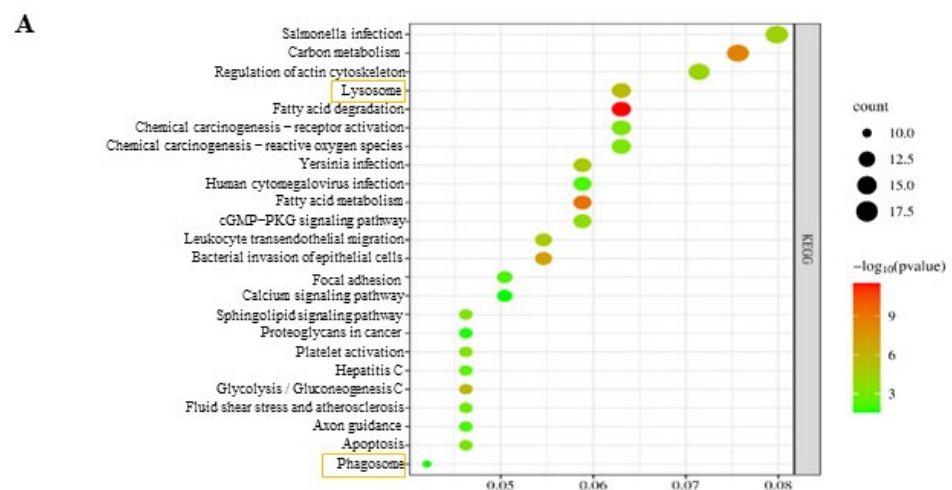


Figure 5. Cont.



**Figure 5.** Quantitative proteome analysis of sperm and testis haploid cells in  $Nrdp1^{+/-}$  and  $Nrdp1^{-/-}$  mice. (A) FACS gating strategy for isolation of haploid cells using Hoechst33342 staining (P2 group). (B) Proteins from testis haploid cells and sperm of  $Nrdp1^{+/-}$  (control) and  $Nrdp1^{-/-}$  (KO) mice were analyzed prior to mass spectrometric detection by SDS-PAGE and silver staining. (C) Differential expressed proteins in testis haploid cells from  $Nrdp1^{+/-}$  and  $Nrdp1^{-/-}$  mice. (D) Up- and downregulated proteins in testis haploid cells from  $Nrdp1^{+/-}$  and  $Nrdp1^{-/-}$  mice. (E) Differential expressed proteins in sperm from  $Nrdp1^{+/-}$  and  $Nrdp1^{-/-}$  mice. (F) Up- and downregulated proteins in spermatozoa from  $Nrdp1^{+/-}$  and  $Nrdp1^{-/-}$  mice. (G) Co-upregulated proteins in both sperm and testis haploid cells from  $Nrdp1^{-/-}$  mice. (H) Upregulated proteins in  $Nrdp1^{-/-}$  mice testis haploid cells and downregulated in  $Nrdp1^{-/-}$  mice sperm. (I) Co-downregulated proteins in both sperm and testis haploid cells in  $Nrdp1^{-/-}$  mice.



**Figure 6.** Cont.

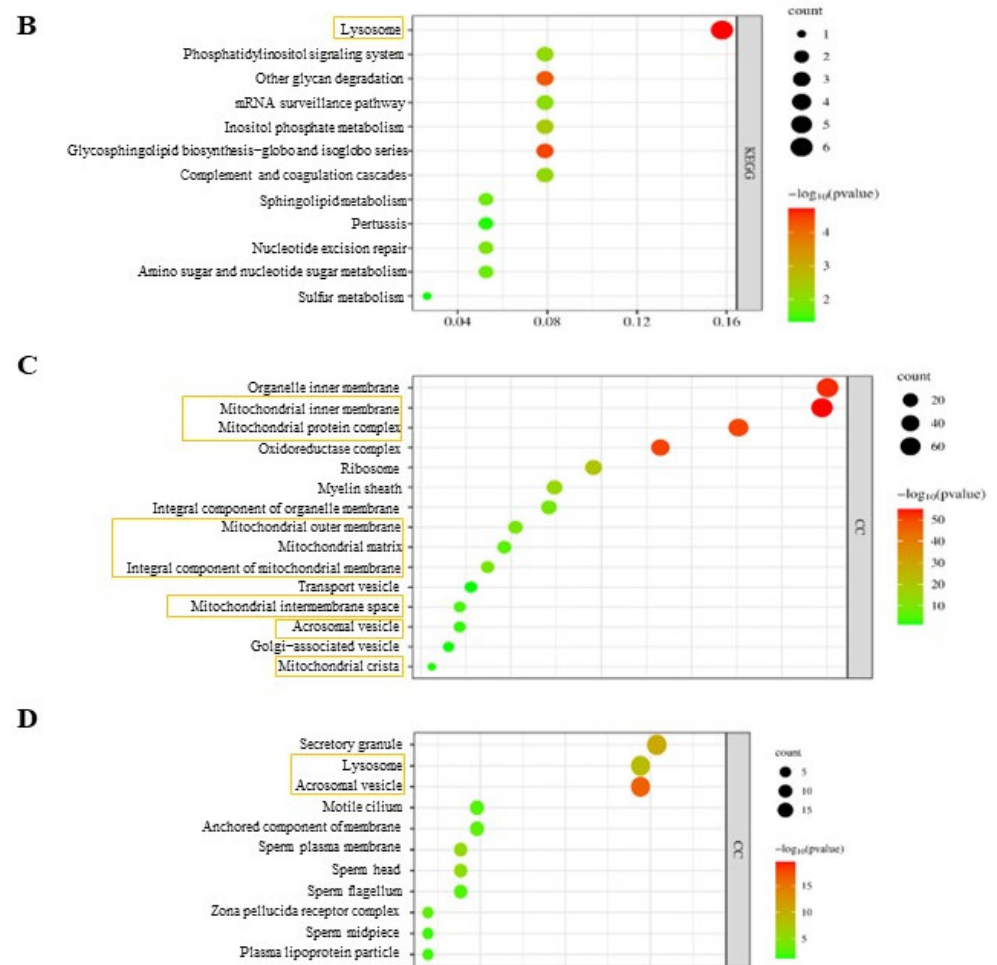


**Figure 6.** Pathway and enrichment analyses in *Nrdp1*<sup>+/-</sup> and *Nrdp1*<sup>-/-</sup> mouse haploid cells in testis or epididymis. (A) KEGG-pathway analysis of the proteins upregulated (440) in *Nrdp1*<sup>-/-</sup> testis haploid cells, colored by *p*-values. (B) KEGG-pathway analysis of the proteins downregulated (113) in *Nrdp1*<sup>-/-</sup> sperm from the epididymis, colored by *p*-values. (C) Cellular component enrichment GO term analysis of upregulated expressed proteins (374) in *Nrdp1*<sup>-/-</sup> sperm, CC: cellular component, colored by *p*-values. (D) Cellular component enrichment GO term analysis of downregulated expressed proteins (113) in *Nrdp1*<sup>-/-</sup> sperm, CC: cellular component, colored by *p*-values. The proceeds and cellular components in yellow boxes stand for which were associated with mitochondria, acrosome and autophagy.

Immunoblotting analyses demonstrated that deletion of *Nrdp1* decreases the levels of the autophagic marker LC3-II, the lysosome membrane protein LAMP1, the vesicle transfer and fusion protein VAMP8 [33], and the autophagic cargo receptor OPTN [34], while increasing the levels of the cargo receptor as well as an autophagic substrate p62 [35] in mouse testes (Figure 7A), suggesting that autophagy is generally inhibited in the *Nrdp1*-deficient testes. Immunoblotting analyses demonstrated that *Nrdp1* deletion obviously increased the levels of Parkin, but decreased the levels of LC3, the mitochondrial fission protein Drp1, the autophagy-promoting protein SIP, and mitochondrial inner membrane protein Tim23 [36] in sperm from the epididymis (Figure 7B), indicating that autophagy is also inhibited in the *Nrdp1*-deficient sperm in the epididymis. The levels of the ubiquitinated proteins at high molecular weights in *Nrdp1*-deficient sperm are slightly higher than those in the wild-type (Figure 7C). But, several ubiquitinated bands at low molecular weights almost disappeared in the *Nrdp1*-deficient sperm. The sizes of these downregulated ubiquitinated proteins are above that of non-ubiquitinated Parkin (52 kDa) (Figure 7C), consistent with the role of *Nrdp1* as a ubiquitin ligase of Parkin [18]. Immunoblotting analyses also showed that

the levels of the acrosomal marker Sp56 [37] decreased in the *Nrdp1*<sup>-/-</sup> sperm from the epididymis (Figure 7D), further supporting that the autophagy-dependent formation of acrosome requires *Nrdp1*. In addition, the deletion of *Nrdp1* shifted the distribution of mitochondrial Parkin and Drp1 from the tail to the head of sperm, accompanying the shifting of mitochondrial localization (Figure 7E,F). These results suggest that *Nrdp1* plays a critical role in mitochondrial localization and function during spermiogenesis at least partially by promoting Parkin ubiquitination. Thus, *Nrdp1* is required for programmed autophagy, acrosome biogenesis, and proper mitochondrial function during spermiogenesis.

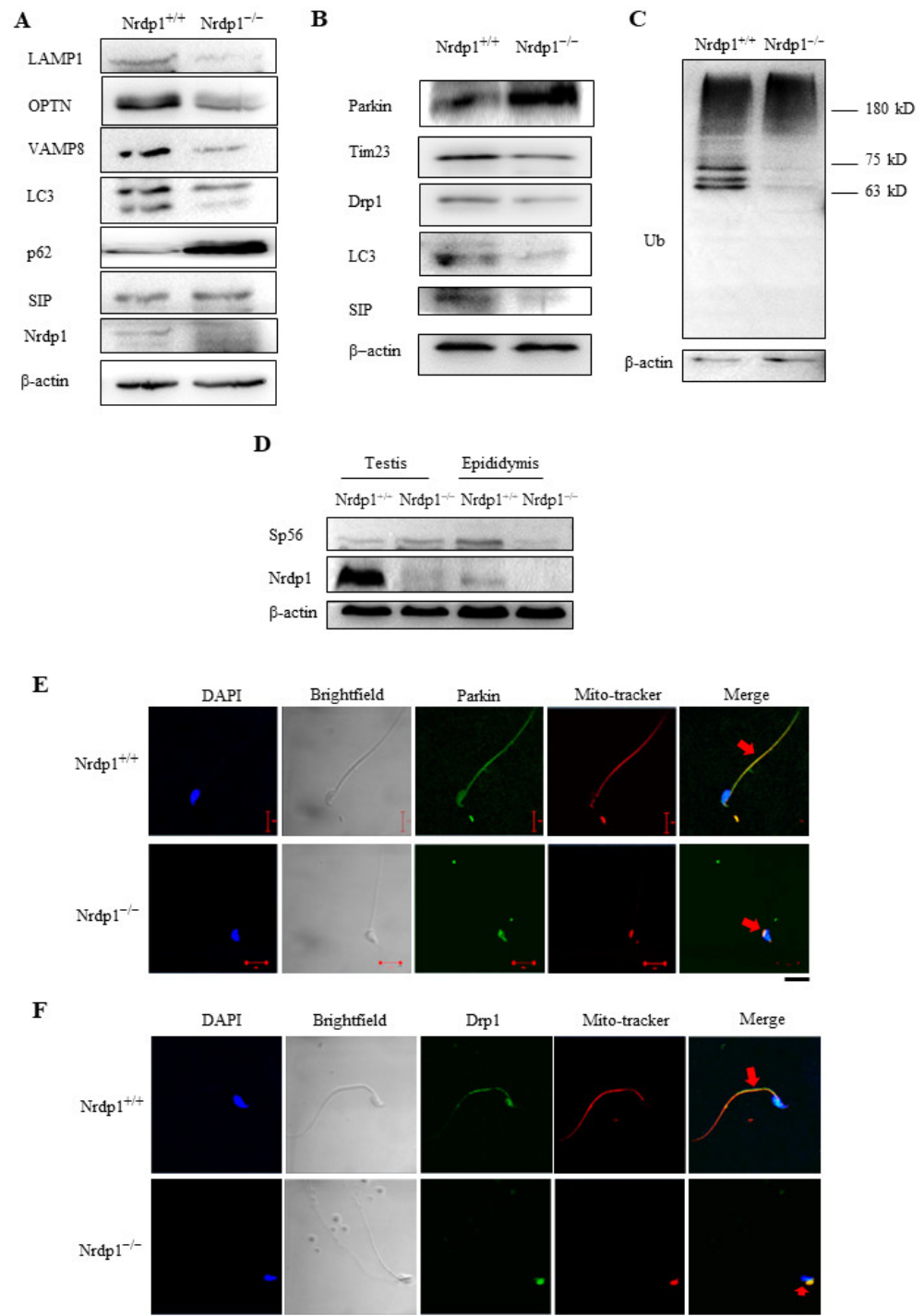


**Figure 7.** *Nrdp1* deficiency disrupts expression or localization of lysosomal or mitochondrial proteins in spermatids and sperm. (A–C) Immunoblotting of the testis (A) or sperm (B,C) homogenates from

*Nrdp1*<sup>+/+</sup> and *Nrdp1*<sup>-/-</sup> mice.  $\beta$ -actin was used as the loading control. (D) Immunoblotting of testis and epididymis homogenates from *Nrdp1*<sup>+/+</sup> and *Nrdp1*<sup>-/-</sup> mice.  $\beta$ -actin was used as the loading control. (E,F) Immunofluorescence analyses of sperm using antibodies against Parkin (E) or Drp1 (F) (green). Mitochondria were stained by MitoTracker (red). The nuclei were stained by DAPI (blue). The red arrows stand for colocalization of Parkin or Drp1 with mitochondria. Scale bar = 10  $\mu$ m. Data are from three independent biological replicates of the same experiment.

#### 4. Discussion

Autophagy plays an important role in sperm acrosome formation [38,39]. Deficiency of the autophagic protein ATG7 in male mouse germ cells leads to the production of round-headed sperm with abnormal acrosome development [11]. The deletion of *Sirt1*, which deacetylates ATG7 and LC3, also leads to similar phenotypes in mouse sperm [40]. The phenotypes of *Nrdp1* deletion were similar to those of the germ cell-specific knockout of *Atg7*, which were apparently due to the inhibition of autophagy, because the levels of the autophagy-promoting protein SIP, the autophagy marker LC3-II, and the mitochondrial inner membrane protein Tim23 were all reduced in sperm by *Nrdp1* deletion. Parkin mutations lead to an autosomal recessive form of Parkinson's disease due to its role in regulating mitophagy for mitochondrial quality control [41]. *Nrdp1* promotes Parkin ubiquitination, and regulates the intracellular activity of Parkin [18], the latter of which promotes ubiquitination and degradation of the mitochondrial fission protein Drp1 [42]. While the levels of the other *Nrdp1* substrates in sperm, including ErbB3 [15] and BIRC6/BRUCE [17], were not elevated by *Nrdp1* deletion (Table S7 [43,44]), this study shows that deletion of *Nrdp1* increased the levels of Parkin, but reduced the levels of Drp1 in sperm, suggesting that the suppressed ubiquitination of Parkin at least partially contributes to the abnormal arrangement of mitochondria in sperm, the impaired sperm motility, and male infertility. Among the substrates of *Nrdp1*, Parkin is the only one upregulated in *Nrdp1*-deficient mice sperm. Thus, Parkin might be the main substrate of *Nrdp1* spermiogenesis through controlling autophagy and mitochondrial quality. Due to the lack of an efficient in vitro sperm culture system, this study did not provide any rescuing data by placing the *Nrdp1* gene back into the *Nrdp1*-deficient sperm. But our quantitative proteome analyses showed that expression of the proteins associated with mitochondria, lysosomes and acrosomes is largely dysregulated in either spermatids or sperm of the *Nrdp1*-deficient mice, validating that the autophagic pathway is indeed affected by deletion of *Nrdp1*. These results are consistent with the known roles of *Nrdp1* in enhancing the association of the pro-autophagy protein SIP/CacyBP with the trans-Golgi network to promote autophagosome formation and promoting the ubiquitin-mediated degradation of the mitophagy-regulating protein Parkin [16,18]. *Nrdp1* exists in both the trans-Golgi network and recycling endosomes, and SIP probably regulates the *Nrdp1*-mediated translocation of BRUCE and LC3-I from the trans-Golgi network to the recycling endosome [16]. Thus, *Nrdp1* should form a complex with BRUCE and LC3-I, which is regulated by SIP. But how this complex is regulated for degrading Parkin during spermiogenesis remains to be determined in the future. The sperm phenotypes of the *Nrdp1*-deficient mice are very similar to those of globozoospermia, a rare reproductive disease characterized by acrosome absence, lack of post-acrosomal sheaths, and abnormal mitochondrial sheaths [45,46].

#### 5. Conclusions

We found that global deletion of *Nrdp1* in mice disrupts mitochondrial arrangement in sperm. During spermiogenesis, *Nrdp1* deletion disrupts acrosome biogenesis and results in round-headed sperm. *Nrdp1* controls the Parkin levels and promotes autophagy in sperm. In conclusion, we have found that the ubiquitin ligase *Nrdp1* is essential for spermiogenesis and male fertility by regulating autophagy. These results may provide new clues to cope with the related male reproductive diseases.

**Supplementary Materials:** The following supporting information can be downloaded at: <https://www.mdpi.com/article/10.3390/cells12182211/s1>, Figure S1: Crispr-Cas9 schematic diagram of *Nrdp1* deletion in mice. Figure S2: No difference in *Nrdp1*-deficient Sertoli cells is detectable. Figure S3: Motility of *Nrdp1*<sup>-/-</sup> sperm is defective. Figure S4: GO-term analysis in *Nrdp1*<sup>+/-</sup> and *Nrdp1*<sup>-/-</sup> mouse sperm; Table S1: Proteins co-upregulated in *Nrdp1*<sup>-/-</sup> sperm and testis haploid cells. Table S2: Proteins upregulated in *Nrdp1*<sup>-/-</sup> testis haploid cells, but downregulated in *Nrdp1*<sup>-/-</sup> sperm. Table S3: Mitochondrion or lysosome-related proteins upregulated in *Nrdp1*<sup>-/-</sup> testis haploid cells. Table S4: Mitochondrion or lysosome-related proteins upregulated in *Nrdp1*<sup>-/-</sup> sperm. Table S5: Acrosome-related proteins downregulated in *Nrdp1*<sup>-/-</sup> testis haploid cells. Table S6: Acrosome-related proteins downregulated in *Nrdp1*<sup>-/-</sup> sperm. Table S7: Expression of partial *Nrdp1* substrates in *Nrdp1*<sup>-/-</sup> sperm; Video S1: Wild-type sperms. Video S2: *Nrdp1*-KO sperms.

**Author Contributions:** Z.-Y.L. devised and performed the experiments except for the mass spectrometric analysis. P.X. and T.Z. carried out proteomic studies. X.-B.Q. and T.-X.J. conceived the project and supervised the experiments. X.-B.Q., Z.-Y.L. and T.-X.J. analyzed data and wrote the manuscript. All authors have read and agreed to the published version of the manuscript.

**Funding:** This work was supported by funding from the Ministry of Science and Technology of China (2019YFA0802100, 2018YFC1003300) and the Beijing Natural Science Foundation (5202014).

**Institutional Review Board Statement:** The animal study was reviewed and approved by the Animal Use and Care Committee of Beijing Normal University.

**Data Availability Statement:** The data that support the findings of this study are available from the authors upon request, and requests for materials should be addressed to X.-B.Q. (xqiu@bnu.edu.cn).

**Conflicts of Interest:** The authors declare no conflict of interest.

## References

- Oakberg, E.F. A description of spermiogenesis in the mouse and its use in analysis of the cycle of the seminiferous epithelium and germ cell renewal. *Am. J. Anat.* **1956**, *99*, 391–413. [[CrossRef](#)]
- Fawcett, D.W. The mammalian spermatozoon. *Dev. Biol.* **1975**, *44*, 394–436. [[CrossRef](#)]
- Hartree, E.F. The acrosome-lysosome relationship. *J. Reprod. Fertil.* **1975**, *44*, 125–126. [[CrossRef](#)] [[PubMed](#)]
- Kang-Decker, N.; Mantchev, G.T.; Juneja, S.C.; McNiven, M.A.; van Deursen, J.M. Lack of acrosome formation in *Hrb*-deficient mice. *Science* **2001**, *294*, 1531–1533. [[CrossRef](#)] [[PubMed](#)]
- Mayorga, L.S.; Tomes, C.N.; Belmonte, S.A. Acrosomal exocytosis, a special type of regulated secretion. *IUBMB Life* **2007**, *59*, 286–292. [[CrossRef](#)] [[PubMed](#)]
- Klionsky, D.J.; Ohsumi, Y. Vacuolar import of proteins and organelles from the cytoplasm. *Annu. Rev. Cell Dev. Biol.* **1999**, *15*, 1–32. [[CrossRef](#)] [[PubMed](#)]
- Mizushima, N.; Klionsky, D.J. Protein turnover via autophagy: Implications for metabolism. *Annu. Rev. Nutr.* **2007**, *27*, 19–40. [[CrossRef](#)]
- Rubinsztein, D.C.; Cuervo, A.M.; Ravikumar, B.; Sarkar, S.; Korolchuk, V.; Kaushik, S.; Klionsky, D.J. In search of an “autophagometer”. *Autophagy* **2009**, *5*, 585–589. [[CrossRef](#)] [[PubMed](#)]
- Kabeya, Y.; Mizushima, N.; Ueno, T.; Yamamoto, A.; Kirisako, T.; Noda, T.; Kominami, E.; Ohsumi, Y.; Yoshimori, T. LC3, a mammalian homologue of yeast Apg8p, is localized in autophagosomal membranes after processing. *EMBO J.* **2000**, *19*, 5720–5728. [[CrossRef](#)]
- Kim, I.; Rodriguez-Enriquez, S.; Lemasters, J.J. Selective degradation of mitochondria by mitophagy. *Arch. Biochem. Biophys.* **2007**, *462*, 245–253. [[CrossRef](#)]
- Wang, H.; Wan, H.; Li, X.; Liu, W.; Chen, Q.; Wang, Y.; Yang, L.; Tang, H.; Zhang, X.; Duan, E.; et al. Atg7 is required for acrosome biogenesis during spermatogenesis in mice. *Cell Res.* **2014**, *24*, 852–869. [[CrossRef](#)] [[PubMed](#)]
- Varuzhanyan, G.; Ladinsky, M.S.; Yamashita, S.I.; Abe, M.; Sakimura, K.; Kanki, T.; Chan, D.C. Fis1 ablation in the male germline disrupts mitochondrial morphology and mitophagy, and arrests spermatid maturation. *Development* **2021**, *148*, 199686. [[CrossRef](#)]
- Smith, D.M. Could a Common Mechanism of Protein Degradation Impairment Underlie Many Neurodegenerative Diseases? *J. Exp. Neurosci.* **2018**, *12*. [[CrossRef](#)]
- Kisselev, A.F. Site-Specific Proteasome Inhibitors. *Biomolecules* **2021**, *12*, 54. [[CrossRef](#)] [[PubMed](#)]
- Qiu, X.B.; Goldberg, A.L. Nrdp1/FLRF is a ubiquitin ligase promoting ubiquitination and degradation of the epidermal growth factor receptor family member, ErbB3. *Proc. Natl. Acad. Sci. USA* **2002**, *99*, 14843–14848. [[CrossRef](#)]
- Jiang, T.X.; Zou, J.B.; Zhu, Q.Q.; Liu, C.H.; Wang, G.F.; Du, T.T.; Luo, Z.Y.; Guo, F.; Zhou, L.M.; Liu, J.J.; et al. SIP/CacyBP promotes autophagy by regulating levels of BRUCE/Apollon, which stimulates LC3-I degradation. *Proc. Natl. Acad. Sci. USA* **2019**, *116*, 13404–13413. [[CrossRef](#)]

17. Qiu, X.B.; Markant, S.L.; Yuan, J.; Goldberg, A.L. Nrdp1-mediated degradation of the gigantic IAP, BRUCE, is a novel pathway for triggering apoptosis. *EMBO J.* **2004**, *23*, 800–810. [[CrossRef](#)]
18. Zhong, L.; Tan, Y.; Zhou, A.; Yu, Q.; Zhou, J. RING finger ubiquitin-protein isopeptide ligase Nrdp1/FLRF regulates parkin stability and activity. *J. Biol. Chem.* **2005**, *280*, 9425–9430. [[CrossRef](#)] [[PubMed](#)]
19. Eiyama, A.; Okamoto, K. PINK1/Parkin-mediated mitophagy in mammalian cells. *Curr. Opin. Cell Biol.* **2015**, *33*, 95–101. [[CrossRef](#)] [[PubMed](#)]
20. Lee, Y.; Lee, H.Y.; Hanna, R.A.; Gustafsson, A.B. Mitochondrial autophagy by Bnip3 involves Drp1-mediated mitochondrial fission and recruitment of Parkin in cardiac myocytes. *Am. J. Physiol. Heart Circ. Physiol.* **2011**, *301*, H1924–H1931. [[CrossRef](#)] [[PubMed](#)]
21. Wu, W.; Lin, C.; Wu, K.; Jiang, L.; Wang, X.; Li, W.; Zhuang, H.; Zhang, X.; Chen, H.; Li, S.; et al. FUNDC1 regulates mitochondrial dynamics at the ER-mitochondrial contact site under hypoxic conditions. *EMBO J.* **2016**, *35*, 1368–1384. [[CrossRef](#)]
22. Diamonti, A.J.; Guy, P.M.; Ivanof, C.; Wong, K.; Sweeney, C.; Carraway, K.L., 3rd. An RBCC protein implicated in maintenance of steady-state neuregulin receptor levels. *Proc. Natl. Acad. Sci. USA* **2002**, *99*, 2866–2871. [[CrossRef](#)]
23. Gaysinskaya, V.; Soh, I.Y.; van der Heijden, G.W.; Bortvin, A. Optimized flow cytometry isolation of murine spermatocytes. *Cytom. A* **2014**, *85*, 556–565. [[CrossRef](#)]
24. Shevchenko, A.; Tomas, H.; Havlis, J.; Olsen, J.V.; Mann, M. In-gel digestion for mass spectrometric characterization of proteins and proteomes. *Nat. Protoc.* **2006**, *1*, 2856–2860. [[CrossRef](#)]
25. Wisniewski, J.R.; Zougman, A.; Nagaraj, N.; Mann, M. Universal sample preparation method for proteome analysis. *Nat. Methods.* **2009**, *6*, 359–362. [[CrossRef](#)]
26. Li, Y.-C.; Hu, X.-Q.; Zhang, K.-Y.; Guo, J.; Hu, Z.-Y.; Tao, S.-X.; Xiao, L.-J.; Wang, Q.-Z.; Han, C.-S.; Liu, Y.-X. Afaf, a novel vesicle membrane protein, is related to acrosome formation in murine testis. *FEBS Lett.* **2006**, *580*, 4266–4273. [[CrossRef](#)]
27. Toshimori, K.; Ito, C. Formation and organization of the mammalian sperm head. *Arch. Histol. Cytol.* **2003**, *66*, 383–396. [[CrossRef](#)]
28. Adams, J. The proteasome: Structure, function, and role in the cell. *Cancer Treat. Rev.* **2003**, *29* (Suppl. S1), 3–9. [[CrossRef](#)] [[PubMed](#)]
29. Stringer, D.K.; Piper, R.C. Terminating protein ubiquitination: Hasta la vista, ubiquitin. *Cell Cycle* **2011**, *10*, 3067–3071. [[CrossRef](#)] [[PubMed](#)]
30. Stringer, D.K.; Piper, R.C. A single ubiquitin is sufficient for cargo protein entry into MVBs in the absence of ESCRT ubiquitination. *J. Cell Biol.* **2011**, *192*, 229–242. [[CrossRef](#)] [[PubMed](#)]
31. Narendra, D.P.; Youle, R.J. Targeting mitochondrial dysfunction: Role for PINK1 and Parkin in mitochondrial quality control. *Antioxid. Redox Signal.* **2011**, *14*, 1929–1938. [[CrossRef](#)] [[PubMed](#)]
32. Carlsson, S.R.; Roth, J.; Piller, F.; Fukuda, M. Isolation and characterization of human lysosomal membrane glycoproteins, h-lamp-1 and h-lamp-2. Major sialoglycoproteins carrying polylactosaminoglycan. *J. Biol. Chem.* **1988**, *263*, 18911–18919. [[CrossRef](#)]
33. Behrendorff, N.; Dolai, S.; Hong, W.; Gaisano, H.Y.; Thorn, P. Vesicle-associated membrane protein 8 (VAMP8) is a SNARE (soluble N-ethylmaleimide-sensitive factor attachment protein receptor) selectively required for sequential granule-to-granule fusion. *J. Biol. Chem.* **2011**, *286*, 29627–29634. [[CrossRef](#)] [[PubMed](#)]
34. Fracchiolla, D.; Sawa-Makarska, J.; Zens, B.; Ruiter, A.; Zaffagnini, G.; Brezovich, A.; Romanov, J.; Runggatscher, K.; Kraft, C.; Zagrovic, B.; et al. Mechanism of cargo-directed Atg8 conjugation during selective autophagy. *eLife* **2016**, *5*, e18544. [[CrossRef](#)] [[PubMed](#)]
35. Yue, Z. Regulation of neuronal autophagy in axon: Implication of autophagy in axonal function and dysfunction/degeneration. *Autophagy* **2007**, *3*, 139–141. [[CrossRef](#)] [[PubMed](#)]
36. Lohret, T.A.; Jensen, R.E.; Kinnally, K.W. Tim23, a protein import component of the mitochondrial inner membrane, is required for normal activity of the multiple conductance channel, MCC. *J. Cell Biol.* **1997**, *137*, 377–386. [[CrossRef](#)]
37. Kim, K.S.; Cha, M.C.; Gerton, G.L. Mouse sperm protein sp56 is a component of the acrosomal matrix. *Biol. Reprod.* **2001**, *64*, 36–43. [[CrossRef](#)]
38. Huang, Q.; Liu, Y.; Zhang, S.; Yap, Y.T.; Li, W.; Zhang, D.; Gardner, A.; Zhang, L.; Song, S.; Hess, R.A.; et al. Autophagy core protein ATG5 is required for elongating spermatid development, sperm individualization and normal fertility in male mice. *Autophagy* **2021**, *17*, 1753–1767. [[CrossRef](#)]
39. Wang, M.; Zeng, L.; Su, P.; Ma, L.; Zhang, M.; Zhang, Y.Z. Autophagy: A multifaceted player in the fate of sperm. *Hum. Reprod. Update* **2022**, *28*, 200–231. [[CrossRef](#)]
40. Liu, C.; Song, Z.; Wang, L.; Yu, H.; Liu, W.; Shang, Y.; Xu, Z.; Zhao, H.; Gao, F.; Wen, J.; et al. Sirt1 regulates acrosome biogenesis by modulating autophagic flux during spermiogenesis in mice. *Development* **2017**, *144*, 441–451.
41. Pickrell, A.M.; Youle, R.J. The roles of PINK1, parkin, and mitochondrial fidelity in Parkinson’s disease. *Neuron* **2015**, *85*, 257–273. [[CrossRef](#)] [[PubMed](#)]
42. Wang, H.; Song, P.; Du, L.; Tian, W.; Yue, W.; Liu, M.; Li, D.; Wang, B.; Zhu, Y.; Cao, C.; et al. Parkin ubiquitinates Drp1 for proteasome-dependent degradation: Implication of dysregulated mitochondrial dynamics in Parkinson disease. *J. Biol. Chem.* **2011**, *286*, 11649–11658. [[CrossRef](#)]

43. Wald, J.H.; Hatakeyama, J.; Printsev, I.; Cuevas, A.; Fry, W.H.D.; Saldana, M.J.; VanderVorst, K.; Rowson-Hodel, A.; Angelastro, J.M.; Sweeney, C.; et al. Suppression of planar cell polarity signaling and migration in glioblastoma by Nrdp1-mediated Dvl polyubiquitination. *Oncogene* **2017**, *36*, 5158–5167. [[CrossRef](#)] [[PubMed](#)]
44. Wang, C.; Chen, T.; Zhang, J.; Yang, M.; Li, N.; Xu, X.; Cao, X. The E3 ubiquitin ligase Nrdp1 ‘preferentially’ promotes TLR-mediated production of type I interferon. *Nat. Immunol.* **2009**, *10*, 744–752. [[CrossRef](#)]
45. Battaglia, D.E.; Koehler, J.K.; Klein, N.A.; Tucker, M.J. Failure of oocyte activation after intracytoplasmic sperm injection using round-headed sperm. *Fertil. Steril.* **1997**, *68*, 118–122. [[CrossRef](#)] [[PubMed](#)]
46. Anton-Lamprecht, I.; Kotzur, B.; Schopf, E. Round-headed human spermatozoa. *Fertil. Steril.* **1976**, *27*, 685–693. [[CrossRef](#)]

**Disclaimer/Publisher’s Note:** The statements, opinions and data contained in all publications are solely those of the individual author(s) and contributor(s) and not of MDPI and/or the editor(s). MDPI and/or the editor(s) disclaim responsibility for any injury to people or property resulting from any ideas, methods, instructions or products referred to in the content.